VI.1. FISCHER-TROPSCH SYNTHESIS: IMPACT OF PRETREATMENT OF ULTRAFINE IRON OXIDE UPON CATALYST STRUCTURE AND SELECTIVITY (Chen-Shi Huang, Liguang Xu, and Burtron H. Davis).

VI.1.1. ABSTRACT

The present study has shown that activation of a high surface area Fe_2O_3 catalyst in CO in a CSTR using tetralin as solvent results in an activity that is three times that of the material that is activated in H_2 or directly in the syngas. Independent of the catalyst activation, similar methane and CO_2 selectivities are obtained. This suggests that the active catalytic phase is the same for the three pretreatments. Since the particle size estimated by XRD shows a variation within 30%, the difference among the activities of the differently activated catalysts can be attributed to differences in the concentration of active sites on the catalyst surface rather than the extent of the surface.

VI.1.2. INTRODUCTION

Pretreatment has a great impact on the compounds present in iron catalysts and on the Fischer-Tropsch (FT) synthesis activity and selectivity. For a catalyst pretreated in hydrogen at 300°C or above, iron may initially be present in the metallic state. However, it converts rapidly to carbidic phases or oxides when exposed to syngas under reaction conditions (VI.1.1-VI.1.6). An oxidic catalysts that is pretreated in CO or directly exposed to syngas may be converted from Fe_2O_3 to low valent oxides or carbides (VI.1.5,VI.1.7,VI.1.8). In these cases, the composition of the iron phases changes with pretreatment and reaction time (VI.1.9-VI.1.11). It has been reported that pretreatment in CO results in a better catalyst than one pretreated in

hydrogen [VI.1.5,VI.1.10,VI.1.11). Many studies have aimed at defining the active iron phase by correlating the structure of the catalyst to FT synthesis activity (VI.1.1,VI.1.2,VI.1.5,VI.1.6,VI.1.9,VI.1.12-VI.1.15). However, there is no clear consensus as to which phase provides the superior activity (VI.1.10,VI.1.11).

Recently, the advantages of slurry phase FT synthesis in handling the large heat of reaction, the ability to use low H_2/CO ratios and the low capital and operation costs have attracted much attention (VI.1.10). In a slurry phase reactor, the presence of solvent may render the effect of pretreatment on iron catalyst structure and on the FT synthesis activity and selectivity quite different from those reported in earlier studies using plug flow reactors. A better understanding the relationships between pretreatment and the FT activity should lead to improvements in process technology.

The present study focuses on the effect of pretreatment on the structure, catalytic activity and selectivity of a high surface area Fe_2O_3 catalysts in a continuously stirred tank reactor (CSTR). Catalyst samples were withdrawn periodically from the reactor and characterized by X-ray diffraction (XRD) and transmission electron microscopy (TEM). The catalyst characterization results are correlated with FT synthesis activity and selectivity.

VI.1.3. EXPERIMENTAL

VI.1.3.a. Catalyst Activation and Syngas Reaction

A process scheme employing a 300 mL continuously stirred tank reactor (CSTR) was used for the present study (Figure VI.1.1). A slurry of 2.2g of ultrafine Fe_2O_3 (United Technologies, surface area 270 m^2/g) in 180 cc of tetralin (Fisher, 99%) was charged into the CSTR. Pretreatment gas (i.e. CO or H_2) or syngas

(H_2/CO=1.03) was introduced and the reactor was pressurized to 105 psig (8 atm absolute). The temperature of the reactor was then increased from the ambient to 260°C at a rate of 1.5°C/min with a gas flow rate of 2.57 L/g-Fe/h (or 5.57 L/g-Fe/h for a H_2/CO = 1.03 mixture) and a stirring rate of 1200 rpm. The reactor was then held at 260°C for 24 hrs. After activation, syngas (H_2/CO= 1.03) was introduced to the reactor at a flow rate of 5.57 L/g-Fe/h. CO and H_2 conversions and gas products selectivity were obtained by analysis of the exit gas using a Carle gas analyzer. During the activation process and the syngas reaction period, a small amount of catalyst was withdrawn from the reactor at several designated times for X-ray diffraction and electron microscopy studies.

VI.1.3.b. Catalyst Characterization

X-ray Diffraction (XRD) Powder X-ray diffraction patterns were obtained using a Philips APD X-ray diffraction spectrometer equipped with a Cu anode and Ni filter operated at 40 kV and 20 mA (CuKα =1.5418 A). A catalyst slurry sample (ca. 6 ml) was discharged from the reactor into a beaker containing 100 ml acetone. After the catalyst particles settled to the bottom, most of the solvent was removed by decanting. The catalyst was washed with two 20 ml portions of acetone. After drying at room temperature under vacuum, the catalyst was transferred to a sample holder for XRD study. Identification of iron phases in the catalyst was accomplished by comparing the XRD pattern of the catalyst sample with those in the standard powder X-ray diffraction file compiled by the joint committee on powder diffraction standards published by the International Center for Diffraction Data.

Transmission Electron Microscopy (TEM) TEM pictures and data were obtained using a Hitachi model H800NA electron microscopy operating at a voltage of

200 kV. The sample were prepared by suspending the catalyst particles withdrawn from the reactor in acetone. An optimum ratio of acetone to catalyst slurry was determined so that the catalyst particles formed a slightly turbid suspension (ca. 2 ml of catalyst slurry in 400 ml acetone). This suspension was constantly agitated in an ultrasonic bath. A drop of the suspension (ca. 7 μl) was placed with a syringe onto a carbon film coated copper grid. After the acetone evaporated, the grid was loaded into the microscope for analysis.

VI.1.4. RESULTS

VI.1.4.a. Activation in CO

Figure VI.1.2 shows the XRD patterns of the Fe_2O_3 catalyst activated in CO for 2, 10 and 24 h. The untreated Fe_2O_3 is amorphous to XRD. According to the manufacture specification, the Fe_2O_3 structure determined by electron diffraction is hematite. After 2 h of reaction in CO at 260°C, the catalyst shows XRD peaks at 2θ = 30.1, 35.4, 43.1, 56.9 and 62.5° that are characteristic of Fe_3O_4 magnetite (Fig 2a). Furthermore, weak doublet peaks can also be observed above 2θ = 60° (e.g. peaks at ca. 2θ = 90°), indicating the presence of Fe_2O_3 magnetite. Two additional peaks at 2θ = 38.0 and 45.0, which are not due to the magnetites, were also observed; these can be attributed to the two most intense peaks of Fe_3C cementite (2θ = 37.8 and 45.1°). The peak at 45.0° is also coincident with the most intense XRD peak of α-Fe. With further conversion in CO, several changes in the XRD pattern of the catalyst can be noted by comparing Figures VI.1.2b (10 h in CO) and VI.1.2c (24 h in CO) with VI.1.2a:

1. The XRD peaks at 2θ = 30, 35, 43 and 62.5° become broad; indicating the formation of new iron phases;
2. a new, weak peak at 31° was observed that, together with the observation in (1) above, suggests that maghemitite Fe_2O_3 is the new phase since maghemite shows XRD peaks near 31, 35, 43 and 62°;
3. the peak at 56.9° decreases with reaction time; this peak can be used as an indication of the presence of Fe_3O_4 magnetite; therefore, the decrease in intensity of the 56.9° peak suggests the disappearance of magnetite phase in the catalyst with reaction time;
4. the XRD intensity of the peaks at 2θ = 38, 43, 45.0 and 73.0° grow with increasing reaction time.

The increase in the intensity of the 38.0 and 45.0 peaks indicate that the Fe_3C and Fe phases increase with reaction time. The increase in the peak intensity at 43° indicates the possible formation of another phase. As mentioned above, magnetite decreased with run time. Therefore, if the XRD peak at 62.5° is solely due to magnetite, it should decrease with run time. Instead, the 62.5° peak increases with run time; this indicates the presence of an iron phase having an XRD peak near 62.5°. This, and the observation of an increase in intensity of the 73° peak with run time, strongly suggests the formation of a new phase, FeO wustite, which increases with run time.

Figure VI.1.3 shows the XRD pattern of the CO activated catalyst following 10 and 48 hrs. in syngas. After 10 hrs of syngas conversion, the XRD pattern (Fig. 3a) shows that magnetite Fe_3O_4 is the major phase; weak lines at 2θ=38.0 and 45.0 still

can be seen. However, the intensity is weaker than that before the introduction of syngas (Fig 2c). This indicates that a portion of the Fe_3C and/or α-Fe, produced by reaction of Fe_2O_3 with CO, has been oxidized to Fe_3O_4 magnetite. Moreover, by comparing Fig. 2c with Fig. 3a, the XRD characteristic of FeO has disappeared completely after 10 hrs. in syngas. Apparently, the presence of syngas caused the transformation of FeO to Fe_3O_4 magnetite. Prolonged reaction in the syngas environment also caused the XRD peaks characteristic of Fe_3C and α-Fe to disappear completely (Fig. 3b). Based on the Fe_3O_4 (311) peak (2θ=35.3°), using the Scherrer equation ($d=\lambda/w_{1/2}\cos\theta$) a mean particle size of 230 Å was estimated for the catalyst after 10 hr syngas reaction . A particle of this size corresponds to a surface area of about 50 m^2/g (calculated by A=6V/d).

Figure VI.1.4 shows a typical TEM picture for the catalyst activated in CO followed by 10 h of syngas reaction. The particle size distribution based on TEM pictures of the sample is presented in Figure VI.1.5. A normal distribution of particle sizes can be seen. An average particle size of about 290 Å (calculated by $((\Sigma d_i^3)/n)^{1/3}$) was obtained. Thus, the mean particle size of the catalyst obtained from TEM data shows good agreement with the one estimated from XRD line broadening (230 Å).

Figure VI.1.6 shows the evolution of CO_2 as a function of the duration of pretreatment of the Fe_2O_3 catalyst in CO. The fraction of CO_2 in the exited gas decreases from 2.5 % after 2 hr to 0.5% after 24 h in CO. This indicates that the reaction of CO with Fe_2O_3 readily occurs at 260°C; this observation agrees with the XRD results which show the presence of Fe_3O_4, Fe_3C and Fe in the sample activated in CO for 2h (Fig 2a). The detection of CO_2 in the exited gas after 24 h of CO

exposure suggests that the conversion of iron oxides to iron carbides is incomplete; this is consistent with the detection of Fe_3O_4 and FeO by XRD in the sample after 24 h of activation in CO (Fig 2c).

The results of syngas conversion for the catalyst activated in CO are presented in Table VI.1.1 Plots of % hydrogen (filled circles) and CO conversions (filled circles) as a function of reaction time are shown in Figure VI.1.7a and VI.1.7b, respectively. Clearly, the H_2 conversion decreases whereas the CO conversion increases with reaction time. Both CO and H_2 conversion, however, level off at 40% and 22%, respectively, after 10 h of reaction time. Consequently, the H_2/CO usage ratio, indicated in Table VI.1.1 column 4, decreases with time to attain a constant value after 10 h of synthesis.

Figure VI.1.8a and VI.1.8b show CO_2 (filled circles) and CH_4 (filled circles) selectivities, as a function of run time. Both selectivities decrease with run time and level off after 10 h. From column 9 of Table VI.1.1, the C_2 alkene/alkane ratio does not change significantly (ca. 10%) with reaction time. The C_3alkene/alkane ratio (column 10) decreases with run time and remains constant after 10 h on stream. Comparing column 9 and 10 with column 4 of Table VI.1.1, it appears that C_2 alkene/alkane ratio is not affected significantly by a change in the H_2/CO usage ratio; however, the other four selectivities and the C_3 alkene/alkane ratio follow the same trend as that of H_2/CO usage.

VI.1.4.b. Activation in H_2

The XRD patterns for the Fe_2O_3 catalyst after 2, 10 and 24 h in H_2 (260°C, 8 atm) show mainly Fe_3O_4 magnetite phase. An additional weak peak indicating the

presence of metallic Fe was also observed for the catalyst pretreated in hydrogen for 24 h. After reduction, the introduction of syngas does not alter the XRD patterns of the catalyst. This suggests that reduction in H_2 of Fe_2O_3 and the following syngas conversion under 8 atm at 260°C results mainly in Fe_3O_4.

Table VI.1.2 summarizes the results of syngas conversion with the Fe_2O_3 catalyst that was activated in H_2. Plots of H_2 and CO conversion (open circles) versus run time are shown in Figure VI.1.7a and VI.1.7b, respectively. The H_2 conversion increases slightly with run time and levels off at about 18% after 10 h on stream. The CO conversion increases slightly from 2 to 24 h and then decreases. Consequently, as shown in column 4 of Table VI.1.2, the H_2/CO usage ratio increases with run time.

Figure VI.1.8a and VI.1.8b also show the selectivity for CH_4 (open circles), and CO_2 (open circles) as a function of run time, respectively. Clearly both selectivities increase with run time.

Indicated in column 9 and 10 of Table VI.1.2, the alkene/alkane ratio for C_2 remains constant during the 48 h period and the alkene/alkane ratio for C_3 increases slightly with time.

VI.1.4.c. Catalyst Activation During Synthesis

Figure VI.1.9 shows the XRD patterns for the catalyst activated in syngas for 2 (A), 10 (B), 24 (C) and 48 h (D). After only 2h in syngas, Fe_3O_4 is the major phase. The weak peaks appearing as a shoulder at 20=35.3, 43 and 63°, indicate the presence of FeO. The FeO phase increases with run time up to 24 h (Fig 9 b and c) and then has disappeared completely after 48 h (Figure VI.1.9d). α-Fe and/or Fe_3C, indicated by the peaks at 38° and 45° can also be seen for the material after 2 h in

syngas. Similar to the trend observed for FeO, α-Fe and/or Fe_3C phases increase with run time to 24 h then disappear after 48 h on stream.

Table VI.1.3 shows the results of CO hydrogenation for the catalyst activated in syngas only. CO (filled squares) and hydrogen (filled squares) conversions are plotted as a function of run time in Figure VI.1.7a and VI.1.7b respectively. The CO and hydrogen conversions increase with run time and level off after 72 h on stream. Thus, from column 4 of Table VI.1.3, the H_2/CO usage ratio decreases with run time and levels off after 10 h.

Figure VI.1.8a and VI.1.8b show respectively the CH_4 (filled squares), and CO_2 (filled squares) selectivities as a function of synthesis time. Both selectivities decrease with run time, and then level off after 24 h.

From column 9 and 10 of Table VI.1.3, one can see that the alkene/alkane ratios for C_2 and C_3 compounds remain constant for the 96 h period.

VI.1.5. DISCUSSION

VI.1.5.a. Effect of Activation Gas on Catalyst Structure

The present study shows that Fe_2O_3 can be partially reduced in CO, in hydrogen or in CO/H_2 mixture. After 10 h of activation, Fe_2O_3 was completely transformed to Fe_3O_4 and other phases. The ease of reduction of Fe_2O_3 to Fe_3O_4 has been well documented, (VI.1.16,VI.1.17) and is expected on the basis of the exothermic nature of the reaction (VI.1.16).

XRD studies conducted in the present work clearly indicate that CO is a better reducing agent, as well as a carburization agent, than H_2 or the H_2/CO mixture. These results are consistent with a static TG/DTA study which showed that CO is better than

H_2 for the reduction of α-Fe_2O_3 (VI.1.16). The incomplete transformation of Fe_2O_3 to iron carbide after 24 hrs. of activation in CO (Fig 2c) is also consistent with a Mössbauer spectroscopic study that showed the presence of magnetite Fe_3O_4 and Fe_5C_2 in an amorphous α-Fe_2O_3 after 24 hrs of activation in CO at 270°C (VI.1.17). However, Zarochak and McDonald have reported a complete transformation of Fe in a Fe-K-Cu (65:0.29:0.6) catalyst to carbidic iron at 280°C and under 200 psig CO during 24 h in a slurry phase autoclave (VI.1.10). The presence of K, which has been reported to accelerate carburization (VI.1.18,VI.1.19), as well as the higher temperature (280 vs 260°C) and pressure (200 vs 105 psig) they used, may explain the difference between their and our results.

The observation of only a small fraction of metallic iron after 24 h activation in H_2 at 260°C is surprising, but this has also been reported (VI.1.17). It is possible that the condenser in the reactor set-up (Figure VI.1.1) which was used to trap tetralin vapor may also condense water vapor during the course of reaction; this water may reoxidize metallic Fe to Fe_3O_4.

VI.1.5.b. Effect of Syngas Reaction on the Catalyst Structure

After 10 h of syngas conversion, the catalysts activated in hydrogen and CO showed only the Fe_3O_4 phase by XRD. The catalyst without preactivation also showed by XRD only Fe_3O_4 after 48 hr on stream; this has been reported for catalysts which showed mainly iron carbide or α-Fe phase after activation (VI.1.10,VI.1.20). This has been attributed to the presence of water vapor, particularly at high conversion. As mentioned in the previous section, the condenser set-up can accumulate relatively large amounts of water. High water vapor pressure in the reactor is thus expected.

This may be one of the reasons for the detection of only Fe_3O_4 phase by XRD in the catalysts after prolonged syngas conversion.

Carbidic phases were often observed in earlier studies of Fe catalysts (VI.1.5,VI.1.8). However, the catalysts in those studies are low surface area material or contain alkali promoters. An outer layer of large particles of catalysts may retard oxidation of carbidic or metallic phase. The alkali promoter which has been reported to accelerate carburization is also expected to stabilize the carbidic phases. Thus in the present study, the use of higher surface area Fe_2O_3 and the lack of alkali promoter in the catalyst, may be the reason for the observation of only Fe_3O_4 by XRD in the catalysts after 10 or more hours of syngas conversion.

The average particle size of Fe_3O_4 was 230, 250 and 310 Å for catalysts activated in CO and in H_2 followed by 10 h syngas conversion, and direct activation in syngas for 48 h, respectively. Therefore, the activation does not significantly impact on the particle size of the catalysts following syngas conversion. The original catalyst material had particles of about 30 Å diameter; therefore, there is about a ten-fold increase in the particle size following pretreatment and/or use for syngas conversion. Samples of the Fe_2O_3 were pretreated in a plug flow reactor at 260°C and 8 atm in hydrogen or carbon monoxide; the surface of the hydrogen pretreated material was 37 m^2/g and the carbon monoxide pretreated material was 95 m^2/g.

VI.1.5.c. Effect of Pretreatment on CO Hydrogenation Selectivity and Activity

From Figure VI.1.8, it appears that in the earlier stages of syngas conversion, the CO_2 and methane selectivities for the catalysts activated in CO or without preactivation are similar and are higher than that of the H_2-activated catalyst.

However, the two selectivities merge after only 10 h of syngas conversion so that the catalysts prepared by the three activation procedures become the same. Thus, for this catalyst the gas(es) used for activation appear to affect the product selectivity primarily in the earlier stage of syngas reaction. The time dependant trend and magnitude of CH_4 and CO_2 for the catalyst activated in CO (Fig 8, filled circles) and without preactivation (Fig 8, filled squares) indicate that they have similar active phases. Furthermore, independent of pretreatment, both CH_4 and CO_2 selectivities merged after 10 h in syngas. This implies that the active sites in the catalysts are similar after 10 h of syngas conversion.

As shown in Figure VI.1.7, the catalysts activated in hydrogen and without preactivation have comparable CO and hydrogen conversion after 24 h on stream. The catalyst activated in CO or without preactivation showed an induction period; however, no induction period was observed for the hydrogen pretreated catalyst. The CO conversion was similar for the catalyst activated in H_2 or that was not pretreated; however, the CO pretreated catalyst has a CO conversion about three times that of the sample activated in syngas or hydrogen. Thus, the present study clearly shows that, for a high surface area Fe_2O_3 in a CSTR using tetralin as solvent, activation in CO produced the most active catalyst for subsequent CO hydrogenation. The results are consistent with the studies of the effect of activation procedure on FT activity for promoted K-Cu-Fe_2O_3 catalysts (VI.1.10,VI.1.11) and for a FeMn catalyst (VI.1.7). The catalyst activated in H_2 has a CO conversion comparable to that of a catalyst without preactivation, and this is in agreement with the results obtained by Dictor and Bell (VI.1.8).

The XRD patterns indicate that Fe_3O_4 is the only crystalline phase present for the catalyst at the point of maximum activity, and this does not depend upon the activation gases. This implies that Fe_3O_4 is the active phase, or that the active phase can not be detected by XRD. However, the fact that, after 2 h in syngas, Fe_2O_3 already has been completely transformed into Fe_3O_4 and that this material shows only minimum activity while a Fe_3O_4 phase that was observed for the catalyst activated in H_2 for 24 h showed a much higher activity, indicates that bulk Fe_3O_4 is not likely to be the active phase for CO hydrogenation. Furthermore, at maximum activity, the particle size of Fe_3O_4 for the catalyst activated in CO was 74% of that for the catalyst activated in hydrogen. The CO conversion for the CO activated catalyst however, was 3 times that of the catalyst activated in hydrogen. Therefore, the presence of an active surface or bulk phase supported on the surface of Fe_3O_4 is likely.

The attainment of a similar selectivity independent of the initial pretreatment in the present study suggests the same, or at least similar active phase(s). It has been proposed that, under reaction conditions, a number of compounds coexist on the surface of an iron catalyst: iron oxides, iron carbides and metallic iron (VI.1.21). Iron carbides have been proposed as the active phase (VI.1.2,VI.1.9), and that the fraction of iron carbides on the catalyst surface determines the activity (VI.1.9). Others, however, have proposed that metallic iron (VI.1.14,VI.1.15), or iron oxides (VI.1.22-VI.1.24) are the active phases. In the present study, the nature of the active sites was not determined. Nevertheless, the present study suggests that a common active phase can be obtained after a period of syngas conversion.

We speculate that the following transformations occur when a Fe_2O_3 catalyst is pretreated in H_2:

$$Fe_2O_3 \text{ ---> } Fe_3O_4 \text{ ---> } Fe \text{ ---> } FeC_x/Fe_xO_y/Fe.$$

Pretreatment of the Fe_2O_3 catalyst in CO or syngas results in the following transformations:

$$Fe_2O_3 \text{ ---> } Fe_3O_4 \text{ ---> } FeC_x/Fe_xO_y/Fe$$

The difference among the activities of catalysts appears to depend upon the concentration of active sites on the surface. Apparently, Fe_2O_3 activated in CO produced the highest concentration of active sites, and therefore results in the highest activity.

VI.1.6. ACKNOWLEDGMENT

The authors acknowledge the financial support of this work by the Department of Energy contract No. DE-AC22-91PC90056 and by the Commonwealth of Kentucky.

VI.1.7. REFERENCES

VI.1.1. Amelse, J. A.; Schwartz, L. H.; and Butt, J. B. *J. Catal.*, **72**, 95 (1981).

VI.1.2. Raupp, G. B. and Delgass, W. N. *J. Catal.*, **58**, 348 (1979).

VI.1.3. Shen, W. M.; Dumesic, J. A.; and Hill, C. G. *Rev. Sci. Instrum.*, **52**, 858 (1981).

VI.1.4. Dry, M. E., "Catalysis-Science and Technology" (Eds J. R. Anderson and M. Boudart), Vol 1, 160-255 (1981).

VI.1.5. Anderson, R. B. in "Catalysis" edited by P. H. Emmett, Van Nostrand-Reinhold, New York, 1956, Vol IV, pp 29-255.

VI.1.6. Satterfield, C. N.; Hanlon, R. T.; Tung, S. E.; Zou, Z.; and Papaefthymiou, G. C. *Ind. Eng. Chem. Prod. Res. Dev.*, **25**, 401-414 (1986).

VI.1.7. Pennline, H. W.; Zarochak, M. F.; Stencel, J. M.; and Diehl, J. R. *Ind. Eng. Chem. Res.*,. **26**, 595-601 (1987).

VI.1.8. Dictor, R. A. and Bell, A. T. *J. Catal.*, **97**, 121-136 (1986).

VI.1.9. Niemantsverdriet, J. W. and Van Der Kraan, A. M. *J. Catal.*, **72**, 385-388 (1981).

VI.1.10. Zarochak, M. F. and McDonald, M. A. *Proceed. Indirect Liquefaction Contractor Meeting*, Dec 1986, Pittsburgh, pp 58-82.

VI.1.11. Bukur, D. B.; Lang, X.; Rossin, J. A.; Zimmerman, W. H.; Rosynek, M. P.; Yeh, E. B.; and Li, C. *Ind. Eng. Chem. Res.*, **28**, 1130-1140 (1989).

VI.1.12. Matsumoto, H. and Bennett, C. O. *J. Catal.*, **52**, 331 (1978).

VI.1.13. Dwyer, D. J. and Hardenbergh, J. H. *J. Catal.*, **87**, 66-76 (1984).

VI.1.14. Dwyer, D. J. and Somorjai, G. A. *J. Catal.*, **52**, 291 (1978).

VI.1.15. Kerbs, H. J.; Bonzel, H. P.; and Gafner, G. *Surface. Sci.*, **88**, 269 (1979).

VI.1.16. Richard, M. A.; Soled, S. L.; Fiato, R. A.; and Derites, B. A. *Mat. Res. Bull.*, **18**, pp 829-833 (1983).

VI.1.17. Berry, F. J. and Smith, M. R. *J. Chem. Soc. Faraday Trans. I*, **85(2)**, 467-477 (1989).

VI.1.18. Pichler, H. and Merkel, H. "US Bureau of Mines Tech. Paper", 718 (1949).

VI.1.19. Vogler, G. L.; Jiang, X.-Z.; Dumesic, J. A.; and Madon, R. J. *J. Catal.*, **89**, 116 (1984).

VI.1.20. Jellinek, M. H. and Frankuchen, I. in "Advance in Catalysis", Vol 1, Academic Press, 279, (1948).

VI.1.21. Niemantsverdriet, J. W.; Flipse, C. F. J.; Van Der Kraan, A. M.; and Van Loef, J. J. *Appl. Surf. Sci.*, **10**, 302-313 (1982).

VI.1.22. Reymond, J. P.; Meriadeau, P.; and Teichner, S. J. *J. Catal.*, **75**, 39-48 (1982).

VI.1.23. Blanchard, F. B.; Raymond, J. P.; Pommier, B.; and Teichner, S. J. *J. Mol. Catal.*, **17**, 171-181 (1982).

VI.1.24. Hofer, L. J. E., in "Catalysis" edited by P. H. Emmett, Van Nostrand-Reinhold, New York, 1956, Vol IV, pp 373-441.

Table VI.1.1

Results of Syngas Reaction for High Surface Area Fe_2O_3 Preptreated in CO[a]

Time (hr)	% Conversion CO	% Conversion H_2	H_2/CO Usage	% Selectivity[b] CH_4	% Selectivity[b] C_2	% Selectivity[b] C_3	% Selectivity[b] CO_2	Alkene/Alkane C_2	Alkene/Alkane C_3
2	12.6	36.3	3.0	21.3	4.3	4.7	40.1	0.32	1.93
10	37.2	24.2	0.68	6.0	2.0	2.7	17.9	0.29	1.15
24	43.1	21.8	0.53	6.3	2.3	3.0	20.4	0.27	0.91
48	39.0	21.8	0.58	6.4	2.0	2.5	17.5	0.26	0.92

[a] Reaction conditions: 260°C, 8 atm., CO/H_2 = 1.03, 3.9 1/g-Fe_2O_3/hr.

[b] Selectivities are based on total CO conversion.

Table VI.1.2

Results of Syngas Reaction for High Surface Area Fe_2O_3 Preptreated in H_2[a]

Time (hr)	% Conversion CO	% Conversion H_2	H_2/CO Usage	% Selectivity[b] CH_4	% Selectivity[b] C_2	% Selectivity[b] C_3	% Selectivity[b] CO_2	Alkene/Alkane C_2	Alkene/Alkane C_3
2	12.2	14.0	1.24	8.1	1.9	2.5	15.9	0.37	1.25
10	13.0	17.6	1.46	7.8	2.7	2.6	18.1	0.36	1.29
24	13.9	18.4	1.43	7.7	2.6	2.7	18.8	0.31	1.30
48	9.5	17.6	2.00	11.4	4.3	3.6	27.6	0.30	1.55

[a] Reaction conditions: 260°C, 8 atm., CO/H_2 = 1.03, 3.9 1/g-Fe_2O_3/hr.

[b] Selectivities are based on total CO conversion.

Table VI.1.3

Results of Syngas Reaction for High Surface Area Fe_2O_3 Preptreated in H_2[a]

Time (hr)	% Conversion CO	% Conversion H_2	H_2/CO Usage	% Selectivity[b] CH_4	% Selectivity[b] C_2	% Selectivity[b] C_3	% Selectivity[b] CO_2	Alkene/Alkane C_2	Alkene/Alkane C_3
3	3.6	5.9	1.77	20.2	6.5	5.6	63.3	0.33	1.21
10	5.4	7.7	1.23	12.2	4.1	3.2	24.3	0.34	1.66
24	9.0	11.0	1.32	8.1	2.7	2.4	15.2	0.37	1.38
54	8.5	10.8	1.38	10.1	2.9	2.4	14.7	0.35	1.61
72	10.9	14.5	1.48	6.7	2.3	2.0	13.3	0.42	2.02
96	11.8	14.5	1.33	7.3	2.3	2.3	14.6	0.43	1.87

[a] Reaction conditions: 260°C, 8 atm., CO/H_2 = 1.03, 3.9 1/g-Fe_2O_3/hr.

[b] Selectivities are based on total CO conversion.

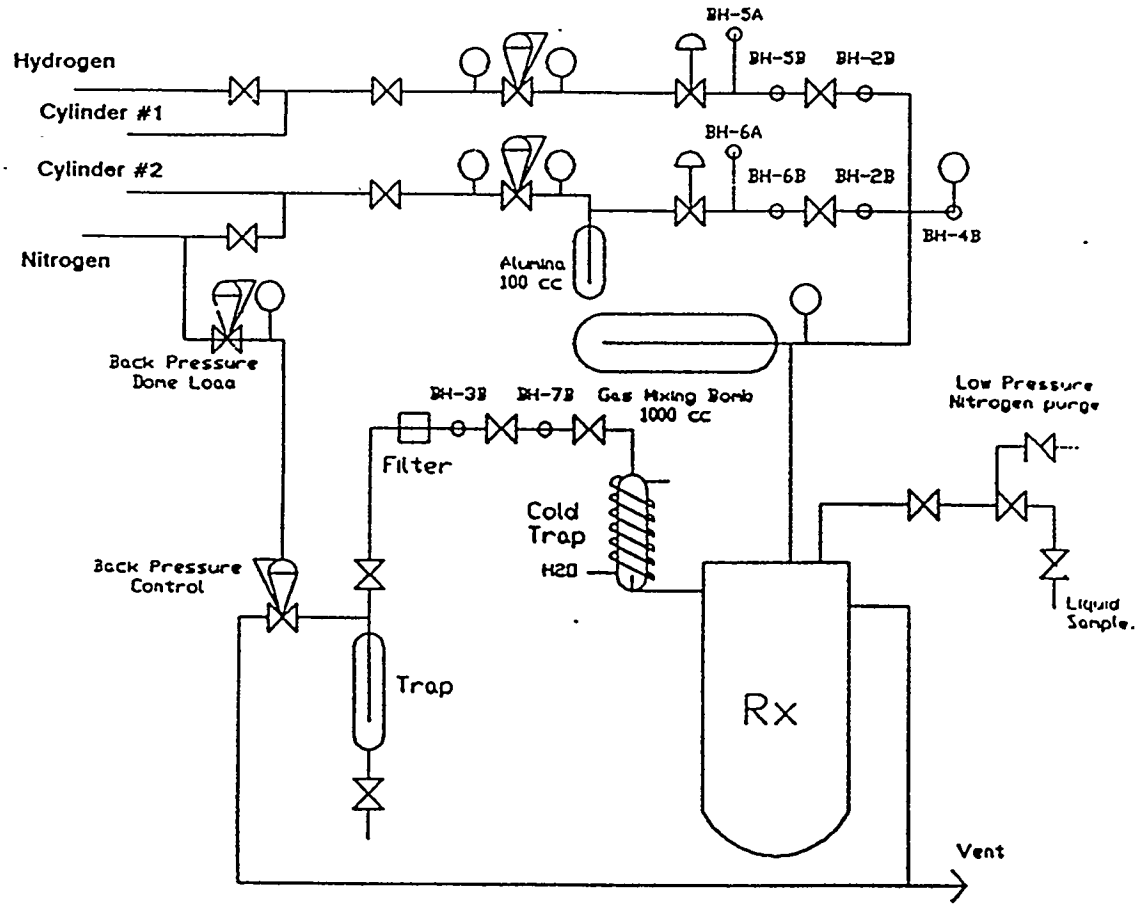

Figure VI.1.1. Flow diagram of the pretreatment/reaction system.

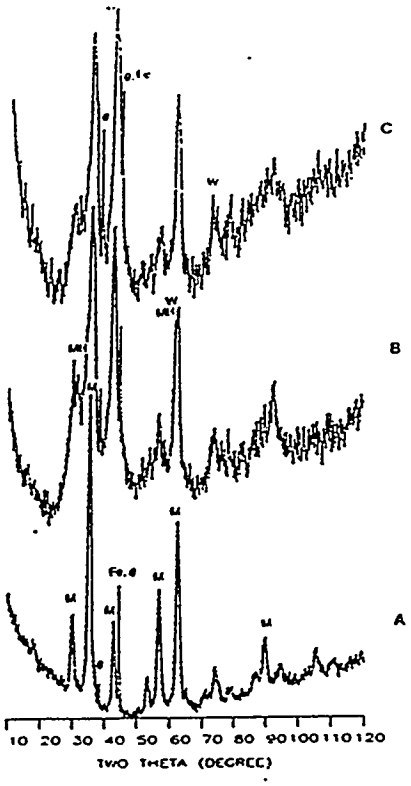

Figure VI.1.2. XRD patterns of the catalyst withdrawn after 2(A), 10(B) and 24 hr. (C) in CO at 8 atm. and 260°C.

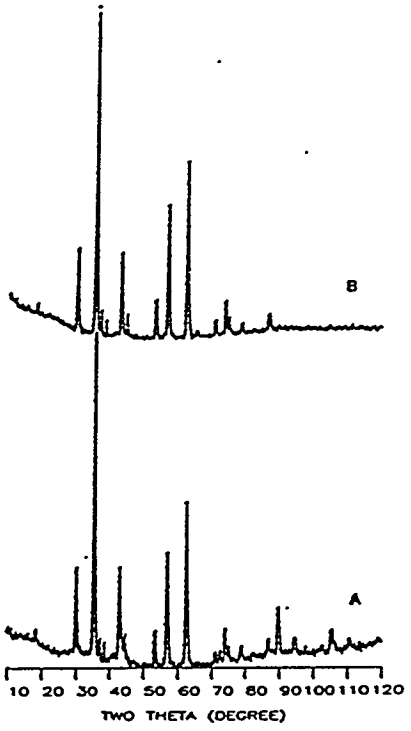

Figure VI.1.3. XRD patterns of the CO pretreated sample (sample represented by figure 2c) following 10(A) and 48 (B) hours in syngas (H_2/CO = 1.03, 8 atm., 260°C).

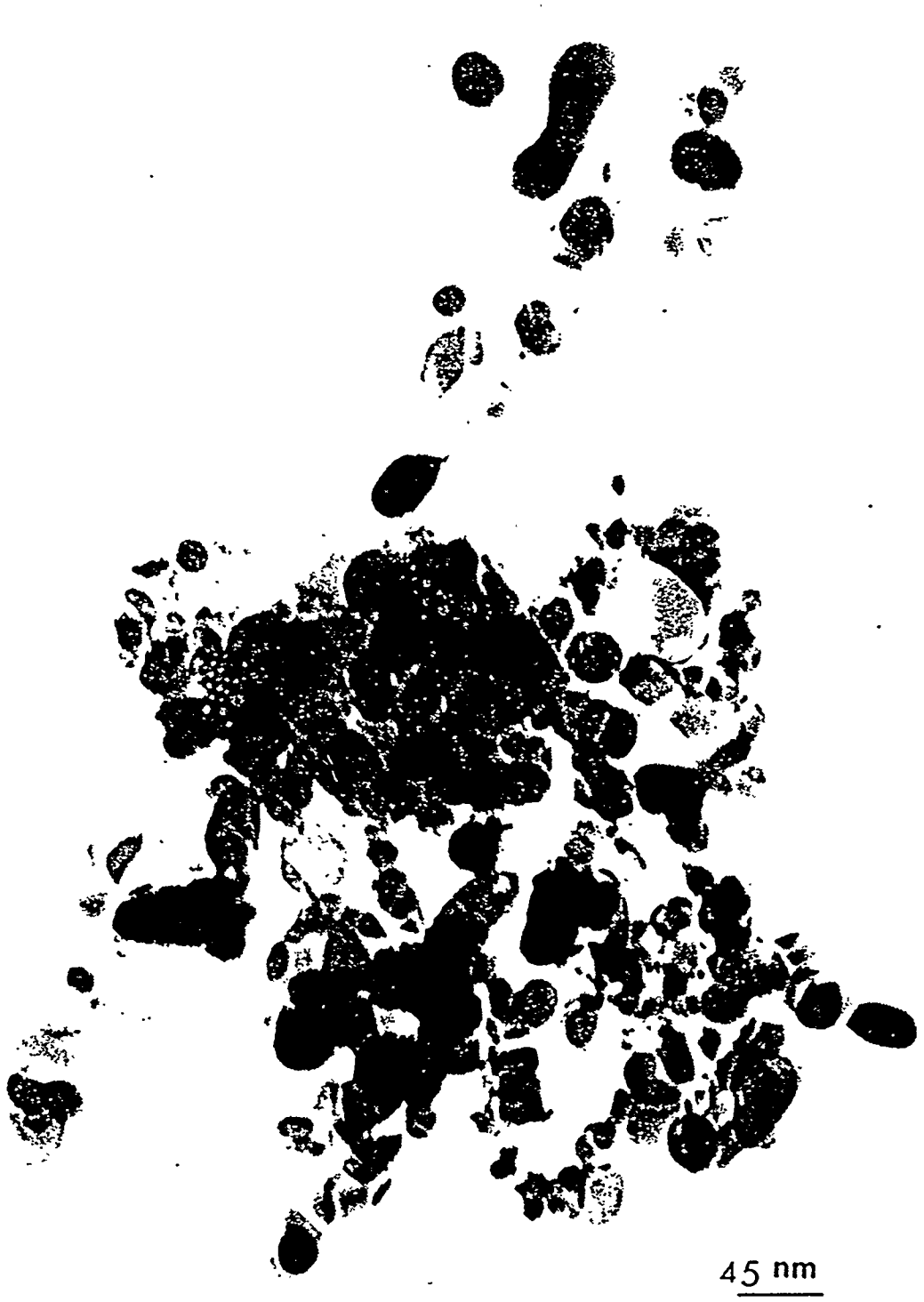

Figure VI.1.4. TEM picture of a catalyst pretreated in CO and exposed to syngas for 10 hours (sample corresponds to Figure 3A).

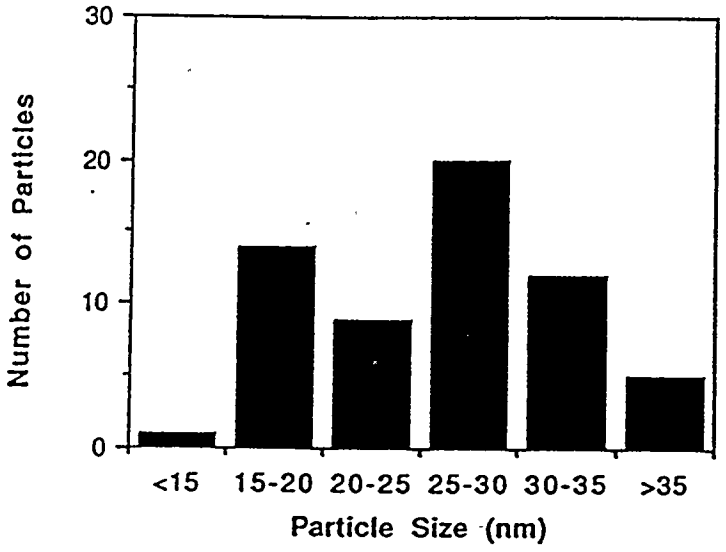

Figure VI.1.5. Size distribution of the particles shown in Figure 3.

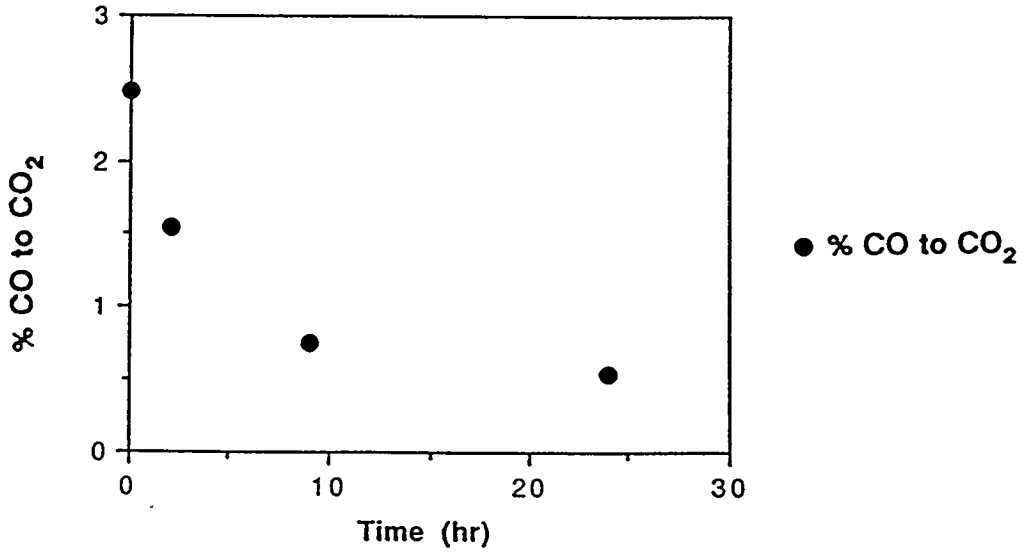

Figure VI.1.6. CO_2 in exit gas during activation in CO at 260°C and 8 atm.

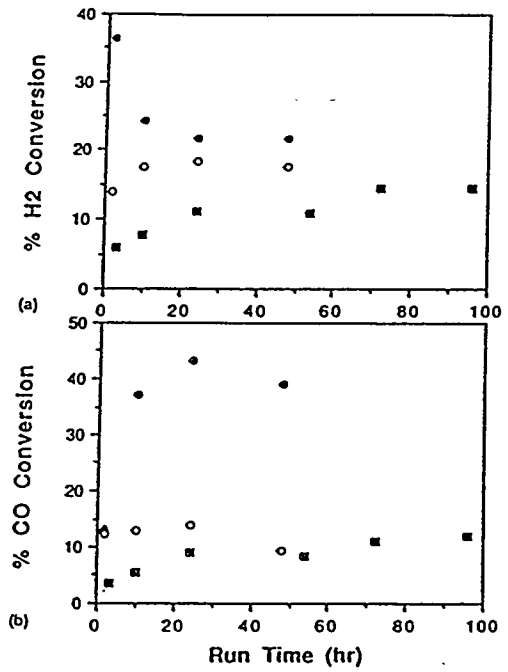

Figure VI.1.7. (top) Hydrogen conversion for the catalyst in CO (●), H_2 (○) or CO/H_2 (■). (bottom) CO conversion for the catalyst activated in CO (●), H_2 (○) or CO/H_2 (■).

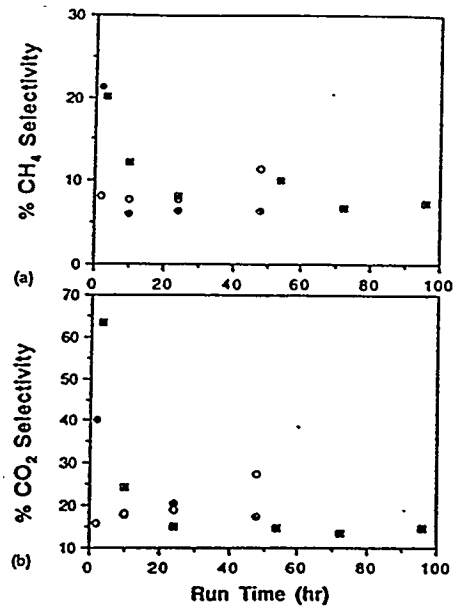

Figure VI.1.8. (top) CO_2 formation for the catalyst activated in CO (●), H_2 (○) or CO/H_2 (■). (bottom) CO_2 formation for the catalyst activated in CO (●), H_2 (○) or CO/H_2 (■).

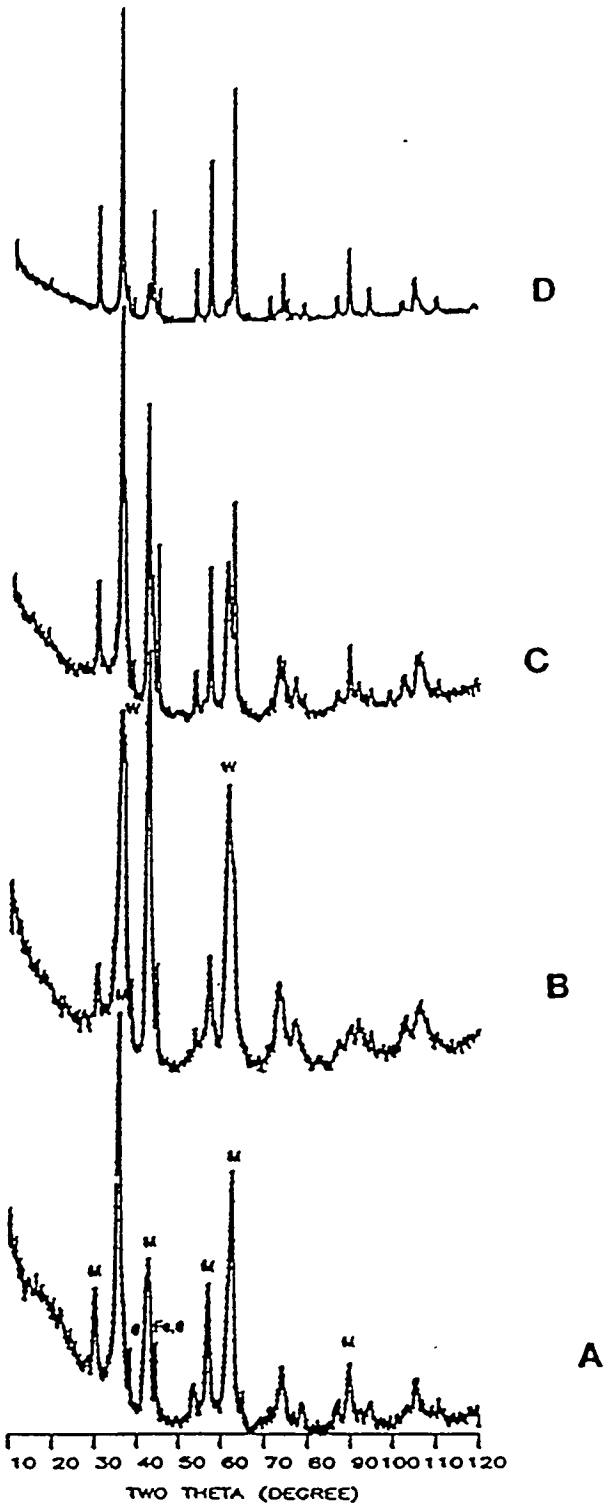

Figure VI.1.9. XRD pattern for the catalyst treated in syngas (CO/H_2 = 1.03) for 2(A), 10(B), 24(C) and 48 hrs. (D) at 260°C and 8 atm.